Supplementary Material

To cross-validate our approach, we acquired higher angular resolution diffusion-weighted MRI (DWI) in a sample of twenty-one healthy control subjects (mean age in years: 40.4±10.1, 15 males) on a Siemens 3.0T Trio scanner. High resolution three-dimensional T1-weighted images were acquired using a MPRAGE sequence (FOV = 250mm; 176 contiguous axial slices; TR/TE = 1900/2.26ms; flip angle = 9^o; voxel size = 1.0 x 1.0 x 1.0 mm). Sixty-eight direction DWI images were acquired using single-shot spin-echo echo-planar imaging (EPI) sequence (FOV = 256 mm; voxel size = 2.0 x 2.0 x 2.0 mm; TR/TE = 9,000/90ms; 69 contiguous axial slices aligned to the AC-PC line collected in 64 directions with b=1000s/mm^2; 4 b0 images without diffusion sensitization).

To generate tractography data, we used PROBTRACKX after applying BEDPOSTX (Bayesian Estimation of Diffusion Parameters Obtained using Sampling Techniques) [Behrens et al., 2007]. BEDPOSTX runs Markov Chain Monte Carlo sampling to build distributions on diffusion parameters at each voxel. It creates all the files necessary for running probabilistic tractography. In our study, up to 3 fibers were modeled per voxel. Once BEDPOSTX had been performed, we chose all voxels with FA≥0.2 as the seeds, and PROBTRACKX was run on each individual seed voxel. PROBTRACKX repeatedly samples from the voxel-wise principal diffusion direction calculated in BEDPOSTX, creating a new streamline at each iteration. This builds a distribution on the likely tract location and path. 1000 iterations were chosen to ensure convergence of the Markov chains, from which the posterior distributions of the local estimate of the fiber orientation distribution were sampled.

We then computed embeddedness in the same Freesurfer defined 82 cortical/subcortical brain regions (Supplemental Table), and correlated them with the corresponding values obtained from our first dataset (which were generated using deterministic tractography). Results showed that highly embedded regions identified in this secondary dataset are consistent with those reported in the main manuscript using the first dataset, and the actual numerical values are highly significantly correlated (P=1.6e-05), despite the fact that they were generated from two different samples using two different tractography reconstruction techniques.

Supplemental Table: Embeddedness values for 82 FreeSurfer cortical/subcortical gray matter regions based on deterministic versus probabilistic tractography

Region Name	Embeddedness for Probabilistic Tractography	Embeddedness for Deterministic Tractography
'ctx-lh-isthmuscingulate'	1.133	0.908
'ctx-rh-rostralanteriorcingulate'	1.045	0.990
'Left-Hippocampus'	0.966	0.653
'ctx-rh-isthmuscingulate'	0.942	1.028
'ctx-rh-caudalanteriorcingulate'	0.924	1.010
'ctx-lh-rostralanteriorcingulate'	0.914	0.920
'ctx-lh-precuneus'	0.876	0.847
'ctx-lh-posteriorcingulate'	0.824	0.893
'ctx-lh-superiorparietal'	0.817	1.011
'ctx-rh-parahippocampal'	0.796	0.571
'ctx-lh-caudalanteriorcingulate'	0.796	0.953
'Right-Hippocampus'	0.796	0.647
'ctx-lh-parahippocampal'	0.795	0.574
'ctx-rh-posteriorcingulate'	0.793	0.972
'ctx-rh-insula'	0.772	0.658
'ctx-lh-insula'	0.765	0.665
'Left-Thalamus-Proper'	0.760	0.910
'ctx-rh-cuneus'	0.758	0.697
'ctx-rh-entorhinal'	0.754	0.542
'ctx-lh-entorhinal'	0.753	0.541
'ctx-rh-medialorbitofrontal'	0.749	0.874
'ctx-lh-medialorbitofrontal'	0.747	0.832
'ctx-rh-precuneus'	0.744	1.019
'ctx-rh-superiorfrontal'	0.736	1.006
'ctx-lh-superiorfrontal'	0.731	1.001
'ctx-lh-cuneus'	0.729	0.742
'Right-Accumbens-area'	0.726	0.767
'ctx-rh-paracentral'	0.723	0.915
'ctx-lh-paracentral'	0.716	0.909
'ctx-rh-postcentral'	0.715	0.743
'ctx-lh-lingual'	0.714	0.611
'ctx-lh-temporalpole'	0.714	0.587
'ctx-lh-parsopercularis'	0.703	0.682
'ctx-rh-frontalpole'	0.702	0.816
'Right-Thalamus-Proper'	0.696	0.920
'Left-Accumbens-area'	0.696	0.751
'ctx-lh-frontalpole'	0.696	0.765
'ctx-rh-parsopercularis'	0.687	0.705

'ctx-lh-rostralmiddlefrontal'	0.683	0.794
'Left-Caudate'	0.678	0.824
'ctx-rh-precentral'	0.676	0.742
'ctx-rh-rostralmiddlefrontal'	0.674	0.808
'ctx-rh-temporalpole'	0.671	0.592
'Right-Putamen'	0.671	0.747
'ctx-lh-parstriangularis'	0.670	0.611
'Left-Putamen'	0.669	0.794
'ctx-rh-lateralorbitofrontal'	0.667	0.697
'ctx-rh-lingual'	0.666	0.558
'ctx-lh-supramarginal'	0.665	0.818
'ctx-lh-pericalcarine'	0.662	0.605
'ctx-rh-superiorparietal'	0.661	1.055
'ctx-lh-precentral'	0.657	0.744
'Left-Amygdala'	0.654	0.597
'ctx-rh-parstriangularis'	0.653	0.638
'ctx-lh-postcentral'	0.652	0.778
'ctx-lh-caudalmiddlefrontal'	0.651	0.764
'Right-Amygdala'	0.646	0.587
'ctx-rh-caudalmiddlefrontal'	0.639	0.793
'ctx-lh-lateralorbitofrontal'	0.630	0.711
'ctx-rh-supramarginal'	0.628	0.717
'ctx-lh-transversetemporal'	0.624	0.614
'Right-Pallidum'	0.623	0.810
'Right-Caudate'	0.623	0.846
'Left-Pallidum'	0.622	0.821
'ctx-rh-pericalcarine'	0.617	0.568
'ctx-lh-inferiorparietal'	0.606	0.814
'ctx-rh-transversetemporal'	0.596	0.587
'ctx-rh-lateraloccipital'	0.595	0.764
'ctx-lh-parsorbitalis'	0.592	0.619
'ctx-lh-fusiform'	0.590	0.598
'ctx-rh-parsorbitalis'	0.583	0.631
'ctx-lh-lateraloccipital'	0.575	0.958
'ctx-rh-superiortemporal'	0.560	0.606
'ctx-lh-superiortemporal'	0.557	0.625
'ctx-rh-inferiorparietal'	0.556	0.763
'ctx-lh-bankssts'	0.556	0.689
'ctx-rh-fusiform'	0.551	0.590
'ctx-rh-bankssts'	0.518	0.624
'ctx-lh-inferiortemporal'	0.509	0.594
'ctx-rh-inferiortemporal'	0.499	0.605
'ctx-lh-middletemporal'	0.492	0.634

'ctx-rh-middletemporal'	0.472	0.628

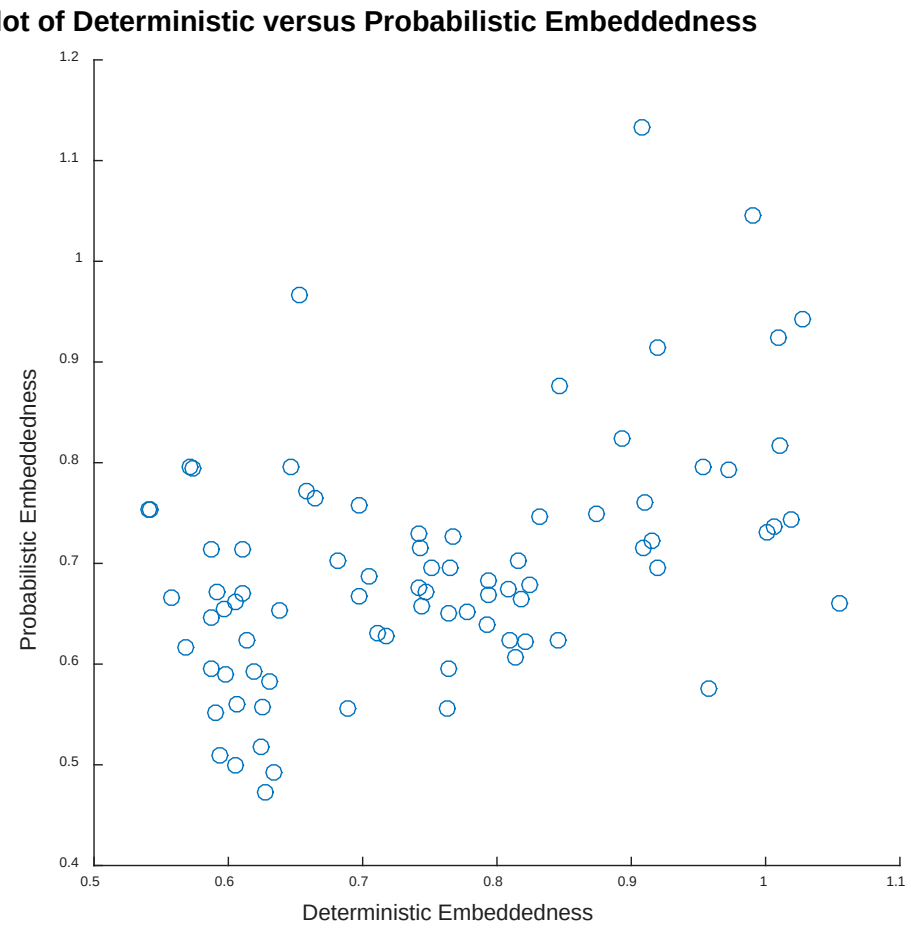

Supplemental Figure. Scatter plot showing the 82 deterministic embeddedness values versus their probabilistic counterparts. R= 0.46, P value=1.6e-05.